



Preparation of amidoxime-functionalized biopolymer/graphene oxide gels and their application in selective adsorption separation of U(VI) from aqueous solution

Shasha Yang¹ · Yiwei Huang¹ · Guolin Huang¹ · Wei Peng¹ · Chenglun Guo¹ · Jeffery Shi²

Received: 30 December 2019 / Published online: 17 March 2020
© Akadémiai Kiadó, Budapest, Hungary 2020

Abstract

The amidoxime-functionalized biopolymer/graphene oxide gels were prepared and their performance in the application of the adsorption separation of uranium (VI) in aqueous solution has been studied. The prepared gels were characterized by using scanning electron microscopy, energy dispersive spectroscopy, Fourier transformed infrared spectra, and X-ray diffraction to determine the microscopic morphology, chemical composition and crystal structure. The adsorption performance of the gels including the effects of solution pH and contact time on the adsorption capacity has been evaluated by a batch adsorption technology. The adsorption isotherms and kinetics were measured, and the experimental data were analyzed and shown to be agreed with the Langmuir isotherm and the pseudo-second-order kinetic model. The results demonstrated that the adsorption process was the rate-limiting step in the separation process.

Keywords Amidoxime · Biopolymer · Uranium · Langmuir · Kinetic

List of symbols

c_0	U(VI) ion concentration in the initial solution (mg L ⁻¹)
c_e	U(VI) ion concentration at equilibrium (mg L ⁻¹)
ΔG°	Change in the Gibbs free energy (J mol ⁻¹)
ΔH°	Change in standard enthalpy (J mol ⁻¹)
K_1	Rate constant (L min ⁻¹)
K_2	Rate constant (g mg ⁻¹ min ⁻¹)
K_d	Distribution constant (mL g ⁻¹)
$K_{d,M}$	Distribution coefficients of the competing metal ion (L g ⁻¹)
$K_{d,U}$	Distribution coefficients of U(VI) (L g ⁻¹)
K_F	Constants of Freundlich model (mg g ⁻¹)
K_L	Constant of Langmuir model (L mg ⁻¹)
m	Weight of adsorbent (g)
n	Freundlich linearity index

q_e	Amount of U(VI) ions adsorbed at equilibrium (mg g ⁻¹)
q_m	Theoretical maximum adsorption capacity per unit weight of the adsorbent (mg g ⁻¹)
q_t	Amount of it at time t (mg g ⁻¹)
R	Universal gas constant (8.314 J mol ⁻¹ K ⁻¹)
ΔS°	Change in standard entropy (J mol ⁻¹ K ⁻¹)
$S_{U/M}$	Distribution selectivity coefficient
T	Temperature (K)
t	Time (s)
v	Volume of the solution (L)

Introduction

Nuclear energy has many benefits advantages our life, however, it has also generated a large amount of uranium-containing wastewater, which is very hazardous and possesses a seriously threat to human being and bio-organisms. Therefore, it has to be managed and treated carefully before being discharged into the environment [1]. Recently, there have been numerous remediation technologies proposed, studied and developed for the removal of uranium, such as chemical precipitation [2], ion exchange processes [3, 4], solvent extraction [5], biological treatment [6], membrane processes [7, 8], and adsorption [9, 10]. Among these approaches,

✉ Guolin Huang
guolinhuang@sina.com

¹ State Key Laboratory of Nuclear Resources and Environment, East China University of Technology, Nanchang 330013, China

² School of Chemical and Biomolecular Engineering, The University of Sydney, Sydney 2006, Australia

adsorption is widely used due to its low cost, high efficiency, and easy-to-operate.

Due to their higher surface area and multiple active sites, nanoparticles have been considered as one of the most suitable efficient adsorbents for the nuclear wastewater treatment application [11]. Graphene oxide (GO) is a type of two-dimensional carbon nanomaterials. A large quantity of oxygen atoms is present on the surface of the GO in the forms of epoxy, hydroxyl, and carboxyl groups, which make GO more soluble in aqueous solution and easier to be chemically modified [12]. However, the use of GO results in irreversible coagulation, which would slow down the process of adsorption and decrease the adsorption capacity. In our previous work [13, 14], chitosan (CS), bovine serum albumin (BSA) and sodium carboxymethyl cellulose (CMC) could graft on to the surface of GO and provide required stability for effective removal of uranium (VI).

Uranium-containing wastewater often contains different coexisting ions such as Nd^{3+} , La^{3+} , Ce^{3+} , Sr^{2+} , Ni^{2+} , Co^{2+} and Ba^{2+} . Therefore, how to improve the selectivity of adsorbents on uranium over other ions in the wastewater is a critical aspect of the application. Amidoxime, one of the most effective chelating groups, has attracted increasing attention for its demonstration of the enhancement on selective adsorption of Uranium [15, 16]. According to recent studies [17–19], amino acids, polyamines and metformin, which contain multiple nitrogen based moieties, can facilitate the binding of the $-\text{COOH}$ or $-\text{OH}$ groups onto biopolymer/graphene oxide gels by hydrogen bonds or acid–base-type electrostatic attraction, transforming the assembly of GO nanosheets into hydrogels. Therefore, it is a reasonable speculation that the amidoxime functionalized biopolymer/GO gels may serve as adsorbents with high selectivity to uranium (VI).

This study focuses on the synthesis of amidoxime-functionalized biopolymer/graphene oxide gels and the assessment of its selectivity adsorption capability of U(VI). The adsorption performance of GO-CS-AO/GO-CMC-AO toward U(VI) under various conditions was evaluated by batch experiments. The effects of initial concentrations, pH value, temperature and contact time, were studied to determine the optimum adsorption conditions. The adsorption isotherms, kinetic models, and thermodynamic parameters of the adsorption process, which is critical for potential application of the adsorbent, were also investigated.

Materials and methods

Materials

Graphite powder (99.85%, average particle size of $\leq 30 \mu\text{m}$) were purchased from Sinopharm Chemical Reagent Co., Ltd

(China). Chitosan (CS) in flake form, with a deacetylation percentage of approximately 90% was purchased from China Chemical Agent Co., Ltd. Sodium carboxymethyl cellulose (CMC, 263.2) was purchased from Aladdin Chemical Reagent CO., Ltd (China). All other chemical agents of analytical reagent grade were used without further purification. The water, which was deionized by a Milli-Q Water Purification system, was used throughout the work. GO were prepared by modified Hummers method. U_3O_8 need to be dried at 105°C for 2 h before the U(VI) stock solution preparing. For preparing stock solution with concentration of 1 mg mL^{-1} , $1.1792 (\pm 0.0001) \text{ g}$ of U_3O_8 was dissolved in a 1000 mL flask with deionized water [14].

Preparation of GO-CMC-AO/GO-CS-AO

GO-CS and GO-CMC gels were prepared by using a similar procedure as described in the literatures [13, 14].

The GO-CS-AO/GO-CMC-AO was prepared from 3-Aminopropyltriethoxysilane (APTES) with amidoxime groups. 200 mg of GO-CS/GO-CMC gels was dispersed in the mixture containing 100 mL absolute ethanol, 5 mL of ammonia and 100 μL APTES. The suspension was stirred at 25°C for 16 h and then the dispersion were filtered and washed alternately with deionized water and pure alcohol for 3 times, respectively. The product was dried in a vacuum oven at 60°C for 12 h.

The acrylonitrile (AN) was pretreated by reflux extraction method. 500 mg of this product was ultrasonic dissolved in 50 mL of dimethyl sulfoxide (DMSO). 0.5 g of azodiisobutyronitrile (AIBN) and 2 mL of purified AN were added in the above solution. Then it was stirred in a 65°C water bath for 72 h. After separating the mixture by centrifugation, the solid phase was washed with DMSO for 3 times followed by washing with deionized water for 5 times. Finally, the product was dried in vacuum at 60°C . The second product was put into a 80 mL mixture of methanol and deionized water (1:1 volume ratio), followed by the addition of 1.08 g of sodium carbonate and 1.40 g of hydroxylamine hydrochloride. Thus made mixture was stirred at 65°C for 36 h and isolated by centrifugation. The filtered solid was washed with deionized water for 5 times and dried in a vacuum oven at 60°C for 12 h. Thus obtained products were referred as GO-CS-AO/GO-CMC-AO gels in the paper.

Adsorption experiments

In each experiment, 10 mg of the adsorbents were added into a 20 mL U(VI) solution with known concentration and pH value in a flask. The pH value was adjusted by 0.1 mol L^{-1} HNO_3 and 0.1 mol L^{-1} NaOH solution. After shaking the flask at a thermostatic shaker bath for 3 h, this mixture was centrifuged at 5000 rpm for 10 min to separate the

suspension from the solution. The concentration of U(VI) in the solution was determined by the arsenazo III method with a visible spectrophotometer at 650 nm. The adsorption amount of U(VI) was calculated according to Eq. (1):

$$q_m = \frac{(C_0 - C_e)v}{m} \quad (1)$$

Characterization

The prepared gels were characterized by the following instruments. The Infrared spectra were obtained using the KBr disc method ($400\text{--}4000\text{ cm}^{-1}$) on a FTIR spectrometer (Nicolet 380, Thermo Scientific Brand, USA). XRD pattern of samples were carried out on D8-A25 (Bruker Instrument Co., Ltd., Germany). The SEM image and the EDS analysis were conducted on Nova Nano scanning electron microscopy 450 (FEI Co., Ltd., USA) and EX-250x (Horiba Co., Ltd., Japan), respectively.

Result and discussion

Characterization of GO-CS-AO/GO-CMC-AO gels

The surface morphologies of GO-CS-AO/GO-CMC-AO revealed by SEM analysis were depicted in Fig. 1. The thicker GO nanosheets was observed in both Fig. 1a, b. It also shows clearly a rough surface containing a large number of wrinkles, which were different from that of GO (not shown). The interconnected pores shown in Fig. 1, enable the solute in the solution to diffuse through the gels, making GO-CS-AO/GO-CMC-AO suitable to the further applications of U(VI) adsorption.

FTIR spectra of GO-CS-AO/GO-CMC-AO were shown in Fig. 2. For GO-CS-AO, the characteristic peaks at 1633 cm^{-1} and 1550 cm^{-1} relate to correspond to the vibrations of -NH_2 group and O=C stretching of the carboxyl group, respectively. The new broad adsorption bands at 1340 cm^{-1} and 1047 cm^{-1} correspond to -CH_2 ,

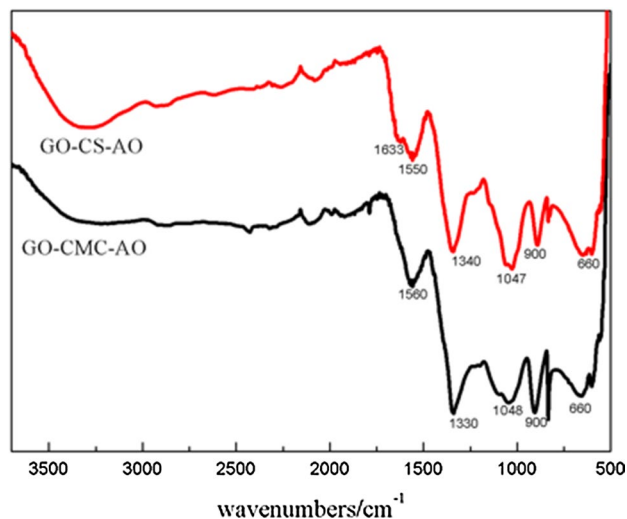


Fig. 2 FTIR spectra of GO-CS-AO and GO-CMC-AO

and C–O–C groups. For GO-CMC-AO, the characteristic peaks at 1560 cm^{-1} and 1330 cm^{-1} belong to -NH_2 in the amidoxime group and the C–O–C groups, respectively. The new peak observed at around 900 cm^{-1} in both GO-CS-AO and GO-CMC-AO is the vibrational absorption peak of the amidoxime group (N–O group). These results confirm the successful formation of GO-CS-AO/GO-CMC-AO gels through cross-linking.

XRD pattern of the samples were measured to further confirm the success of synthesis procedure. As shown in the Fig. 3, the characteristic diffraction peak of GO at 12.2° decreased, and the diffraction peak of chitosan at $2\theta = 23^\circ$ has weakened in Fig. 3 (right), the diffraction peak (at 12.2°) disappeared and a sharp peak (at 21.6°) was observed from Fig. 3 (left), indicating existence of typical crystalline structure of cellulose. All these changes in the XRD patterns suggest that GO was transformed to GO-CS-AO/GO-CMC-AO successfully.

The SEM–EDS analysis along with elemental mapping was carried out for U(VI)-loaded GO-CS-AO/GO-CMC-AO and the images were shown in Fig. 4. Based on the EDS analysis, U (VI) ions had been adsorbed onto the

Fig. 1 SEM images of GO-CS-AO (a) and GO-CMC-AO (b)

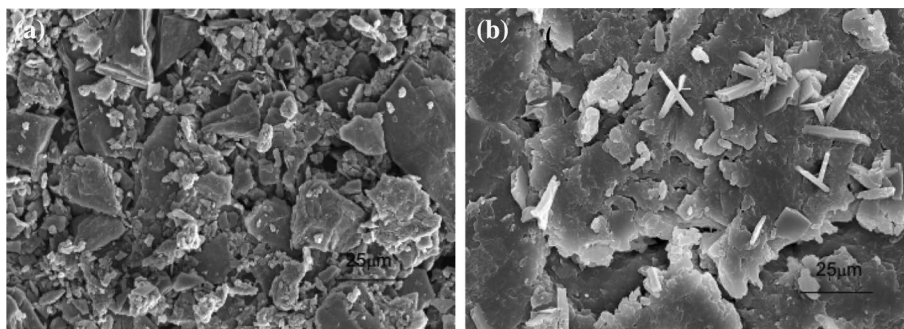


Fig. 3 XRD pattern of GO-CS-AO (right) and GO-CMC-AO (left)

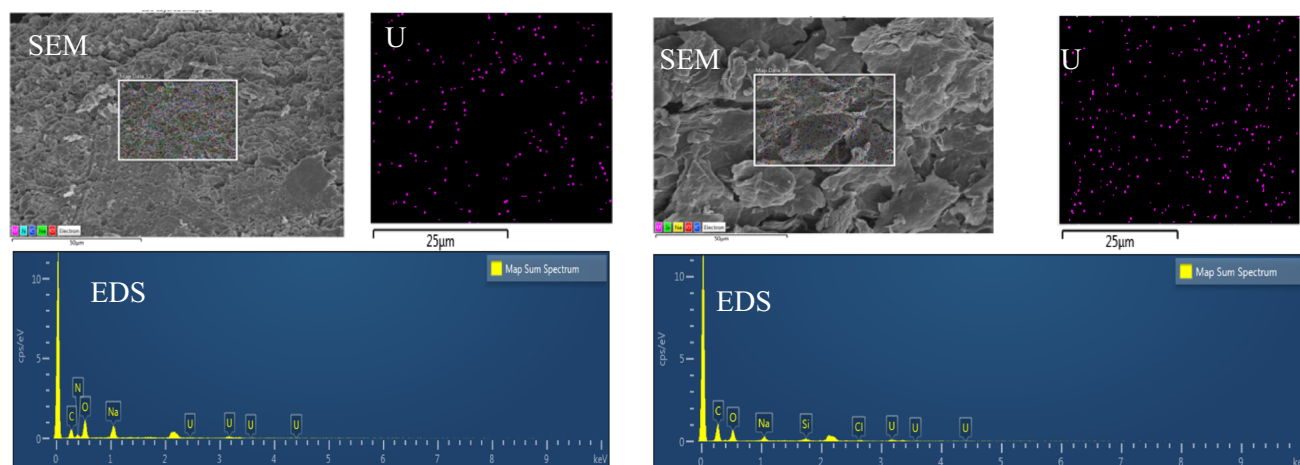
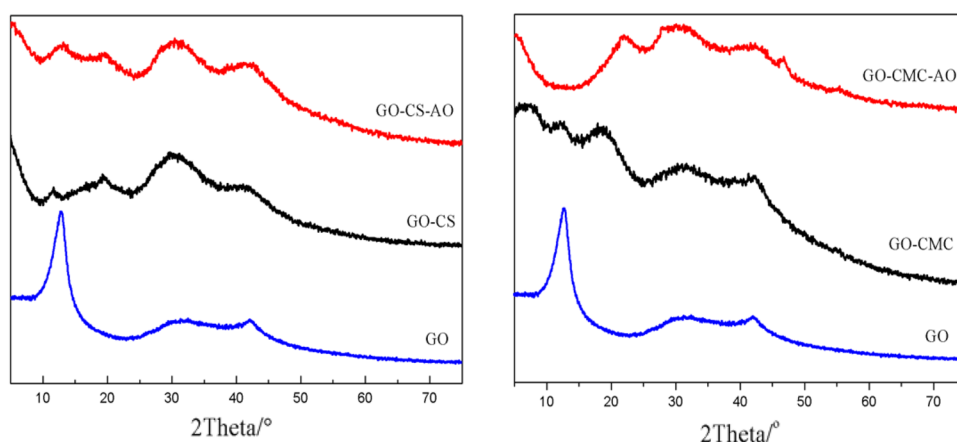


Fig. 4 SEM-EDS mapping of U(VI)-loaded GO-CS-AO (left), GO-CMC-AO (right) of selected area

GO-CS-AO/GO-CMC-AO successfully. Figure 4 shows the SEM with EDS spectra of O and C which are principle components of the gels. Moreover, it was clearly observed from the mapping images that uranium was uniform distributed in the gels.

Effect of pH on adsorption

The pH may affect the U(VI) species distribution and the acid–base properties of the sorbent, and therefore, influences the affinity to U(VI). The results of pH (range from 3.5 to 6.5) effect on the adsorption process with the initial U(VI) concentration of 100 mg L^{-1} at 298 K are shown in Fig. 5. The U(VI) adsorption capacity of GO-CS-AO/GO-CMC-AO increased dramatically as the pH value increased. It is due to the variation of uranium speciation and the changes of adsorbent surface charges at different pH conditions. A relatively high concentration of H^+ at lower pH value leads to the increasing competition between H^+ and the positive uranium species such as UO_2^{2+} , $\text{UO}_2(\text{OH})^+$, and

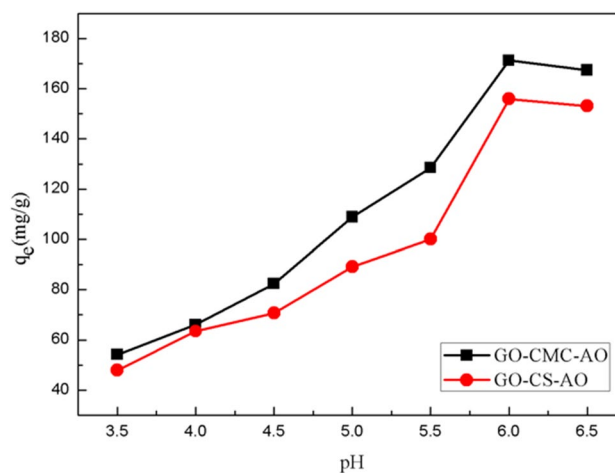


Fig. 5 Effect of pH on adsorption

$(\text{UO}_2)_3(\text{OH})^{5+}$ for the available adsorption sites. Thus, it would protonate the carboxyl and hydroxyl groups of the GO sponge and GO-biopolymer gels to form $-\text{COOH}$ and $-\text{OH}$ groups. With increasing pH value, the reducing concentration of H^+ results in the conversion of the $-\text{COOH}$ and $-\text{OH}$ into $-\text{COO}^-$ and $-\text{O}^-$ groups, respectively. The negative charged groups create the electrostatic attraction between GO-CS-AO/GO-CMC-AO surface and the cationic uranium species. Moreover, the adsorption capacity of U(VI) slightly decreased at pH of 6.5 since the further increased pH value will lead electrostatic between the ions. As a result, the optimal pH of 6.0 was selected in the subsequent experiments.

Adsorption kinetics

The adsorption kinetics is closely related to the contact time. Kinetic studies were performed at 288, 298, 308 K respectively. The effect of the contact time has been investigated over the range from 5 to 180 min with the initial U(VI) concentration of 100 mg L^{-1} at pH of 6.0, the results were plotted in Fig. 6. As shown, the adsorption capacity of U(VI) increases with increasing contact time. The capacity levels

off at contact time of between 120 min and 180 min at all different temperatures. Hence, 120 min appears to be the optimum contact time and would be used for all the consequent experiments.

The pseudo-first-order rate equation and the pseudo-second-order rate equation were applied to assess the experimental data of U(VI) ions adsorbed onto GO-CS-AO/GO-CMC-AO gels to determine the adsorption mechanism. These two rate equations can be expressed as follows:

$$\ln(q_e - q_t) = \ln q_e - K_1 t \quad (2)$$

$$\frac{t}{q_t} = \frac{1}{q_e} t + \frac{1}{K_2 q_e^2} \quad (3)$$

The pseudo-second-order model (t/q_t vs. t) generated by using nonlinear methods was shown in the inset of Fig. 6. The corresponding data of pseudo-first-order model ($\ln(q_e - q_t)$ vs. t , not shown) and the pseudo-second-order model are summarized in Table 1.

From Table 1, the correlation coefficient (R^2) value of pseudo-second-order kinetic model is significantly larger than

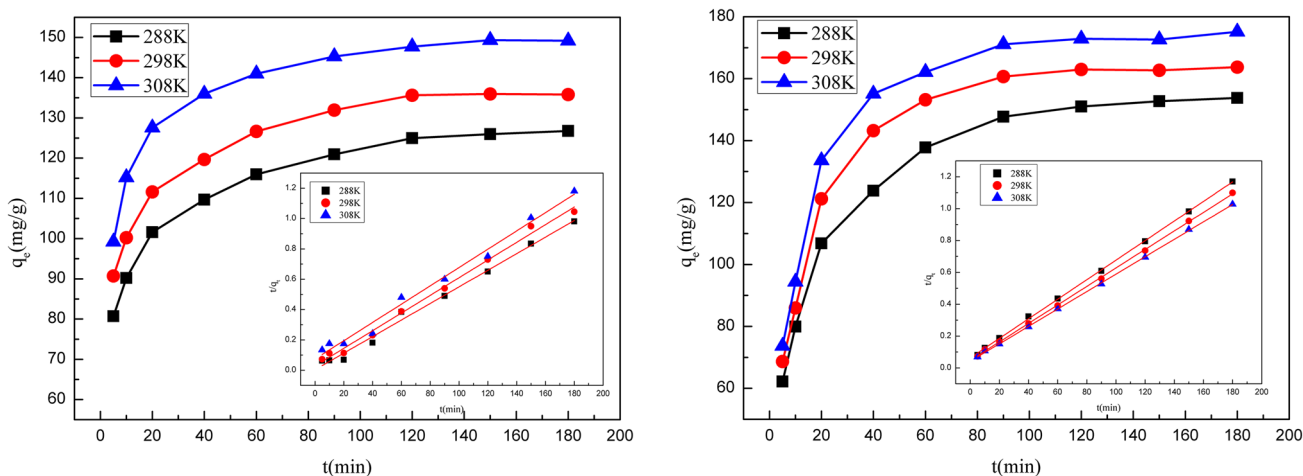


Fig. 6 Effect of Contact time on adsorption capacity for GO-CS-AO (left) and GO-CMC-AO (right); Inset shows the linearized pseudo-second-order plot

Table 1 Kinetic parameters for the pseudo-first-order and pseudo-second-order models

Adsorbents	T (K)	C_0 (mg L^{-1})	$q_{e,\text{exp}}$ (mg g^{-1})	Pseudo-first-order			Pseudo-second-order		
				K_1 (min^{-1})	$q_{e,\text{cal}}$ (mg g^{-1})	R^2	K_2 (mg min^{-1})	$q_{e,\text{cal}}$ (mg g^{-1})	R^2
GO-CS-AO	288	100	126.7	3.54	322.5	0.838	4.96	165.56	0.990
	298	100	135.78	2.42	184.0	0.905	4.23	171.52	0.993
	308	100	149.17	3.10	263.0	0.852	4.45	181.56	0.986
GO-CMC-AO	288	100	153.64	3.06	290.5	0.763	6.02	162.86	0.983
	298	100	163.68	2.86	265.1	0.834	7.14	172.11	0.995
	308	100	175.80	3.22	321.6	0.920	7.15	182.81	0.998

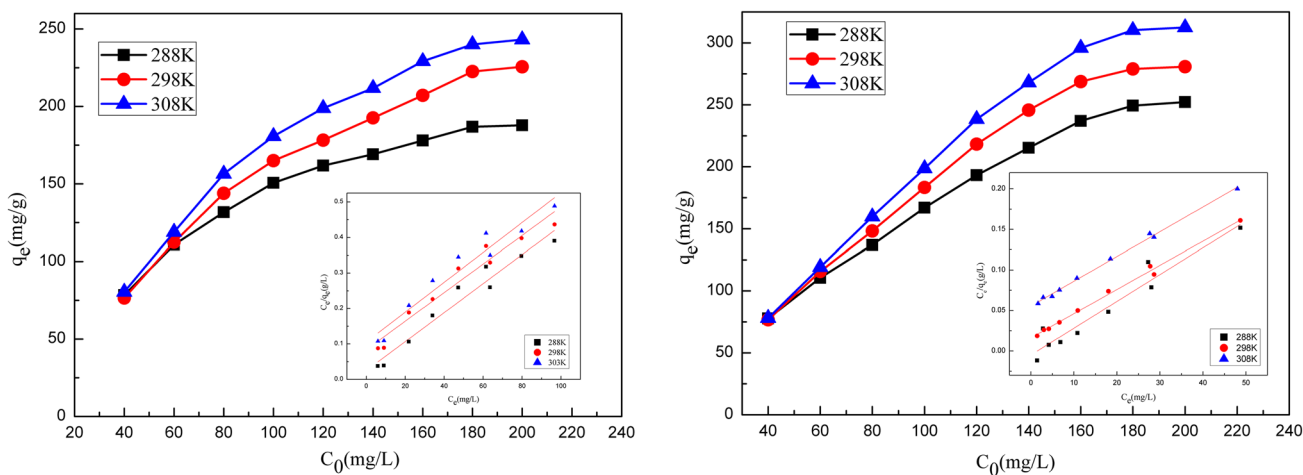


Fig. 7 Effects of initial concentration on adsorption capacity for GO-CS-AO (right) and GO-CMC-AO (left); Inset shows the linearized Langmuir plot

that of pseudo-first-order kinetic model. Therefore, it indicates that pseudo-second-order kinetic model fits the experimental data better than the pseudo-second-order models, as illustrated in the insets of Fig. 6. The data in Table 1 indicate that the current adsorption process might be considered as chemisorption and is rate-limiting step.

Effects of initial ions concentration on adsorption

In adsorption processes, the equilibrium isotherm studies for predicting the behavior of U(VI) ions adsorption onto the adsorbent surfaces are necessary and critical. The obtained experimental data were nonlinearly regressed by using the Langmuir and Freundlich isotherm models as expressed in the following equations:

$$\frac{C_e}{q_e} = \frac{C_e}{q_m} + \frac{1}{q_m K_L} \quad (4)$$

$$\ln q_e = \ln K_F + \frac{1}{n} \ln C_e \quad (5)$$

The C_e versus q_e of U(VI) on GO-CS-AO/GO-CMC-AO is plotted in Fig. 7. The adsorption capacity approached saturation level gradually, and the adsorption amount increased with the increasing initial concentration. The Langmuir isotherm (C_e vs. C_e/q_e) on GO-CS-AO/GO-CMC-AO for the adsorption process are plotted in the inset in Fig. 7. As shown, the Langmuir model fit the adsorption data very well, suggesting a monolayer coverage on both adsorbents.

The corresponding parameters calculated from the two isotherms models are summarized in Table 2. It shows high correlation coefficient, indicating that Langmuir and Freundlich models are applicable and the adsorption of U(VI) onto GO-CS-AO/GO-CMC-AO surface undergoes a process of monolayer coverage. The Langmuir isotherm model was found to fit the adsorption data better based on the value of correlation coefficient. Estimated from the Langmuir model, the maximum capacity of U(VI) absorbed onto GO-CS-AO is 248.75 mg g^{-1} which is lower than that of GO-CMC-AO (327.86 mg g^{-1}).

The batch adsorption results of U(VI) ions removed by reported adsorbents are listed in Table 3. As shown, the maximum adsorption capacity of GO-CS-AO/GO-CMC-AO are higher than the reported results, indicating that they are two

Table 2 Constants in Langmuir and Freundlich isotherms

Adsorbents	T (K)	$q_{m,exp}$ (mg g^{-1})	Langmuir			Freundlich		
			$q_{m,cal}$ (mg g^{-1})	K_d (L mg^{-1})	R^2	K_F (mg g^{-1})	n	R^2
GO-CS-AO	288	187.27	238.25	0.015	0.981	15.03	2.35	0.897
	298	225.95	245.09	0.016	0.993	11.55	2.60	0.905
	308	243.36	248.75	0.023	0.996	14.60	2.56	0.913
GO-CMC-AO	288	260.85	302.11	0.152	0.993	75.92	2.38	0.904
	298	286.85	315.57	0.178	0.993	78.63	2.60	0.935
	308	306.98	327.86	0.182	0.996	77.64	2.78	0.962

Table 3 Comparison of the U(VI) removed by various adsorbents

Material	pH	Temp. (K)	Equilibrium time (min)	Adsorption capacity (mg g ⁻¹)	References
GO@chitosan	5.0	313	150	204.1	[13]
GO@cellulose	5.0	303	150	101.0	[20]
UiO-66@amidoxime	5.5	313	800	227.8	[21]
Mesoporous silica @ amidoxime	5.0	298	120	277.3	[16]
GO-CS-AO/GO-CMC-AO	6.0	308	120	248.75/327.86	This study

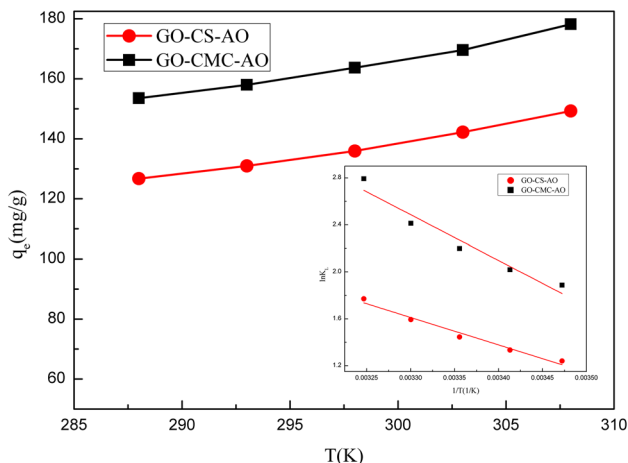


Fig. 8 Van't Hoff plots for the uptake of U(VI)

highly effective adsorbents. Therefore, these two adsorbents could achieve enhanced adsorption selectivity of U(VI) from wastewater containing coexisting ion.

Effects of temperature on adsorption

Thermodynamic considerations of an adsorption process are necessary to determine whether the process is spontaneous or not. The relationship among standard enthalpy (ΔH°), standard entropy (ΔS°) and Gibbs free energy (ΔG°) were described by Eqs. (6) and (7):

$$\ln K_L = -\frac{\Delta H^\circ}{RT} + \frac{\Delta S^\circ}{R} \tag{6}$$

$$\Delta G^\circ = \Delta H^\circ - T\Delta S^\circ \tag{7}$$

The Van't Hoff plots shown in Fig. 8 were used to determine the values of ΔH° and ΔS° based on Eq. (6). The values of ΔH° and ΔS° could be obtained from the slope and intercept of Fig. 8 ($\ln K_d$ vs. $1/T$). Moreover, based on the value of ΔH° and ΔS° , the value of ΔG° was calculated by using Eq. (7). The thermodynamic parameters of the adsorption isotherms at 288, 293, 298, 303 and 308 K are listed in Table 4. The decrease of ΔG° value with the rising temperature demonstrates a more energetically favorable adsorption at higher temperatures. The positive values of ΔH° suggest that these two adsorptions are endothermic reactions, which are consistent with the effect of temperature. Some structural changes, caused by the displacement of adsorbed water molecules occurred during the adsorption process. The positive values of ΔS° implies the increasing disorderness and randomness with increasing at the solid-solution interface. All the above mentioned

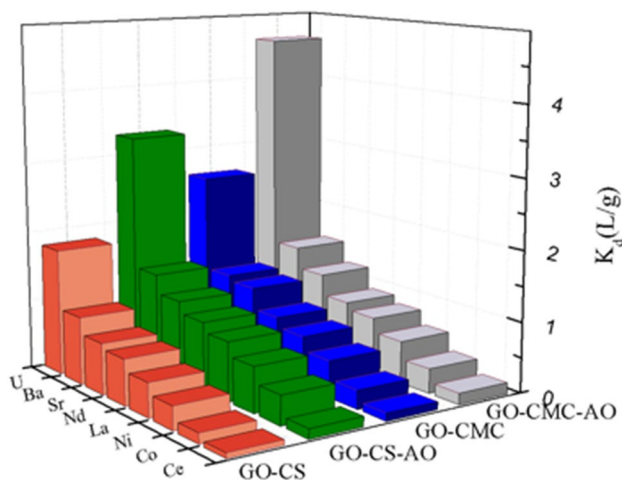


Fig. 9 Selective adsorption of U(VI) on GO-CS, GO-CS-AO, GO-CMC, and GO-CMC-AO

Table 4 Thermodynamic parameters of U(VI) adsorption at different temperature

Adsorbents	ΔH° (kJ mol ⁻¹)	ΔS° (J mol ⁻¹ K ⁻¹)	ΔG° (kJ mol ⁻¹)				
			288 K	293 K	298 K	303 K	308 K
GO-CS-AO	22.69	143.52	-18.64	-19.36	-20.08	-20.79	-21.51
GO-CMC-AO	28.73	156.37	-16.30	-17.09	-17.87	-18.65	-19.43

thermodynamic characteristics reflects the affinity of the GO-CS-AO/GO-CMC-AO towards the U(VI).

Adsorption selectivity

The selective adsorption of GO-CS-AO/GO-CMC-AO for U(VI) ion with the coexistence of Nd^{3+} , La^{3+} , Ce^{3+} , Sr^{2+} , Ni^{2+} , Co^{2+} and Ba^{2+} ions has been investigated with the $m/V = 0.5 \text{ g L}^{-1}$, $C_0 = 100 \text{ mg L}^{-1}$ for a single metal ion at pH of 6.0. The adsorption process of U(VI) and the seven competing cations on GO-CS-AO/GO-CMC-AO are described according to their distribution coefficients (K_d). The distribution selectivity coefficient ($S_{U/M}$) were calculated as follows:

$$K_d = \frac{C_0 - C_e}{C_e} \times \frac{V}{m} \quad (8)$$

$$S_{U/M} = \frac{k_{d,U}}{k_{d,M}}. \quad (9)$$

Figure 9 shows the distribution coefficients of U(VI) and coexist ions on GO-CS, GO-CS-AO, GO-CMC, and GO-CMC-AO. As shown, the adsorption capacity of U(VI) ions on GO-CS-AO/GO-CMC-AO composites is much higher than those of other metal ions. Such outstanding selectivity is mainly attributed to the grafted groups (the $-\text{NH}_2$, $-\text{N}-\text{OH}$ moiety). The $-\text{NH}_2$, $-\text{N}-\text{OH}$ moiety contribute directly to the adsorption of U(VI) ions on GO-CS-AO/GO-CMC-AO composites. Compared with GO-CS/GO-CMC, the highly selective adsorption resulted from the plentiful amino groups of amidoxime in GO-CS-AO/GO-CMC-AO. It supports the conclusion that amidoxime functionalization adopted in this study is effective and that GO-CS-AO/GO-CMC-AO exhibits desirable selectivity for U(VI) over a range of coexisting metal ions.

Regeneration studies

The regeneration of adsorbent is important in commercial implementations. 0.1 M HNO_3 was used as desorption agent in this study. Figure 10 shows the adsorption efficiency of the adsorbent after one to four adsorption/desorption cycles. As shown in Fig. 10, with increasing number of cycles, the adsorption capacities of U(VI) on the GO-CS-AO/GO-CMC-AO decreased gradually. The removal efficiency remained at over 90% of the initial value after four cycles, and then it decreased from the fifth cycle. Therefore, the good performance of the regenerated GO-CS-AO/GO-CMC-AO adsorbents makes them suitable for U(VI) adsorption.

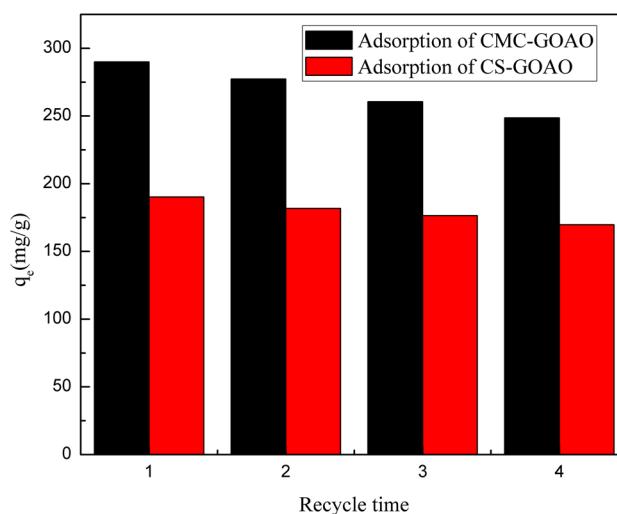


Fig. 10 Effect of recycling adsorbents of GO-CMC and GO-CMC-AO

Conclusions

In conclusion, the preparation of amidoxime-functionalized biopolymer/graphene oxide gels and their application for U(VI) adsorption separation from aqueous solution were investigated in this study. The analysis results of FTIR, XRD, SEM, and EDS indicated that the GO-CS-AO/GO-CMC-AO were synthesized successfully. The factors which affect the U(VI) adsorption were studied by batch experiments, and solution pH of 6.0 and contact time of 120 min were found to be the optimum conditions for U(VI) adsorbed onto GO-CS-AO/GO-CMC-AO. As compared to Freundlich model, Langmuir model demonstrated better description of the adsorption progress. The results indicated that the homogeneous solid surface of the synthesized gels with the regular monolayer adsorption of U(VI). The adsorption kinetics followed the pseudo-second-order rather than pseudo-first-order kinetic model. The parameters of the adsorption thermodynamics calculated from the temperature dependent isotherms suggested that the adsorption process was endothermic and spontaneous. The adsorption selectivity was evaluated by comparing the adsorption efficiencies of single ion solution with that of solution containing coexisting ions.

Acknowledgements The present work was partially supported by the National Science Foundation of China (21866005), Jiangxi Key Plan of Research and Development (20192BBH80011) and the item of State Key Laboratory of Nuclear Resources and Environment (NRE 1611).

Compliance with ethical standards

Conflict of interest The authors declare that they have no conflict of interest.

References

1. He Y, Lin XY, Yan TS, Zhang XN, Luo XG (2018) Selective adsorption of uranium from salt lake-simulated solution by phenolic-functionalized hollow sponge-like adsorbent. *J Chem Technol Biotechnol* 49(2):455–467
2. Chen QY, Yao Y, Li XY, Lu J, Zhou J, Huang ZL (2018) Comparison of heavy metal removals from aqueous solutions by chemical precipitation and characteristics of precipitates. *J Water Process Eng* 26:289–300
3. Banerjee C, Dudwadkar N, Tripathi SC, Gandhi PM, Grover V, Kaushik CP, Tyagi AK (2014) Nano-cerium vanadate: a novel inorganic ion exchanger for removal of americium and uranium from simulated aqueous nuclear waste. *J Hazard Mater* 280:63–70
4. Kim M-J (2001) Separation of inorganic arsenic species in groundwater using ion exchange method. *Bull Environ Contam Toxicol* 67(1):46–51
5. Vázquez-Campos X, Kinsela AS, Collins RN, Neilan BA, Waite TD (2017) Uranium extraction from a low-grade, stockpiled, non-sulfidic ore: impact of added iron and the native microbial consortia. *Hydrometallurgy* 167:81–91
6. Bhat SV, Melo JS, Chaugule BB, D'Souza SF (2008) Biosorption characteristics of uranium(VI) from aqueous medium onto *Catenella repens*, a red alga. *J Hazard Mater* 158(2):628–635
7. Rana D, Matsuura T, Kassim MA, Ismail AF (2013) Radioactive decontamination of water by membrane processes—a review. *Desalination* 321:77–92
8. Luo W, Xiao G, Tian F, Richardson JJ, Wang YP, Zhou JF, Guo JL, Liao XP, Shi B (2019) Engineering robust metal–phenolic network membranes for uranium extraction from seawater. *Energy Environ Sci* 12(2):607–614
9. Chen X, Zhou SK, Zhang LM, You TT, Xu F (2016) Adsorption of heavy metals by graphene oxide/cellulose hydrogel prepared from NaOH/Urea aqueous solution. *Materials* 9(7):582
10. Liu HJ, Zhou YC, Yang YB, Zou K, Wu RJ, Xia K, Xie SB (2019) Synthesis of polyethylenimine/graphene oxide for the adsorption of U(VI) from aqueous solution. *Appl Surf Sci* 471:88–95
11. Rouf TB, Kokini JL (2016) Biodegradable biopolymer–graphene nanocomposites. *J Mater Sci* 51(22):9915–9945
12. Wang Y, Li ZH, Wang J, Li JH, Lin YH (2011) Graphene and graphene oxide: biofunctionalization and applications in biotechnology. *Trends Biotechnol* 29(5):205–212
13. Huang GL, Peng W, Yang SS (2018) Synthesis of magnetic chitosan/graphene oxide nanocomposites and its application for U(VI) adsorption from aqueous solution. *J Radioanal Nucl Chem* 317(1):337–344
14. Peng W, Huang GL, Yang SS, Guo CL, Shi J (2019) Performance of biopolymer/graphene oxide gels for the effective adsorption of U(VI) from aqueous solution. *J Radioanal Nucl Chem* 322:861–868
15. Wang FH, Li HP, Liu Q, Li ZS, Li RM, Zhang HS, Liu LH, Emelchenko GA, Wang J (2016) A graphene oxide/amidoxime hydrogel for enhanced uranium capture. *Sci Rep-UK* 6:19367
16. Zhao YG, Li JX, Zhang SW, Wang XK (2014) Amidoxime-functionalized magnetic mesoporous silica for selective sorption of U(VI). *RSC Adv* 4(62):32710–32717
17. Anirudhan TS, Suchithra PS (2008) Synthesis and characterization of tannin-immobilized hydrotalcite as a potential adsorbent of heavy metal ions in effluent treatments. *Appl Clay Sci* 42(1):214–223
18. Liu Y, Zhao ZP, Yuan DZ, Wang Y, Dai Y, Zhu Y, Chew JW (2019) Introduction of amino groups into polyphosphazene framework supported on CNT and coated Fe₃O₄ nanoparticles for enhanced selective U(VI) adsorption. *Appl Surf Sci* 466:893–902
19. Zhuang ST, Cheng R, Kang M, Wang JL (2018) Kinetic and equilibrium of U(VI) adsorption onto magnetic amidoxime-functionalized chitosan beads. *J Clean Prod* 188:655–661
20. Yang A, Wu J, Huang CP (2018) Graphene oxide-cellulose composite for the adsorption of Uranium(VI) from dilute aqueous solutions. *J Hazard Toxicol Radioact Waste* 22:65–73
21. Liu JM, Yin XH, Liu T (2018) Amidoxime-functionalized metal-organic frameworks UiO-66 for U(VI) adsorption from aqueous solution. *J Taiwan Inst Chem E* 95:416–423

Publisher's Note Springer Nature remains neutral with regard to jurisdictional claims in published maps and institutional affiliations.